Hindawi
Mathematical Problems in Engineering
Volume 2020, Article ID 2609674, 11 pages
https://doi.org/10.1155/2020/2609674

Research Article

Optimal Capacity Allocation of Energy Storage System considering Uncertainty of Load and Wind Generation

Leijiao Ge,[1] Shuai Zhang ,[2] Xingzhen Bai,[2] Jun Yan,[3] Changli Shi,[4] and Tongzhen Wei[4]

[1]*Key Laboratory of Smart Grid of Ministry of Education, Tianjin University, Tianjin 300072, China*
[2]*School of Electrical and Automation Engineering, Shandong University of Science and Technology, Qingdao 266590, China*
[3]*Concordia Institute for Information Systems Engineering, Concordia University, Montréal H3G 1M8, Canada*
[4]*Institute of Electrical Engineering, Chinese Academy of Sciences, Beijing 100190, China*

Correspondence should be addressed to Shuai Zhang; 17864217918@163.com

Received 23 December 2019; Revised 23 March 2020; Accepted 30 March 2020; Published 21 April 2020

Academic Editor: Adrian Chmielewski

Energy storage systems (ESSs) are promising solutions for the mitigation of power fluctuations and the management of load demands in distribution networks (DNs). However, the uncertainty of load demands and wind generations (WGs) may have a significant impact on the capacity allocation of ESSs. To solve the problem, a novel optimal ESS capacity allocation scheme for ESSs is proposed to reduce the influence of uncertainty of both WG and load demands. First, an optimal capacity allocation model is established to minimize the ESS investment costs and the network power loss under constraints of DN and ESS operating points and power balance. Then, the proposed method reduces the uncertainty of load through a comprehensive demand response system based on time-of-use (TOU) and incentives. To predict the output of WGs, we combined particle swarm optimization (PSO) and backpropagation neural network to create a prediction model of the wind power. An improved simulated annealing PSO algorithm (ISAPSO) is used to solve the optimization problem. Numerical studies are carried out in a modified IEEE 33-node distribution system. Simulation results demonstrate that the proposed model can provide the optimal capacity allocation and investment cost of ESSs with minimal power losses.

1. Introduction

The high penetration of wind generations (WGs) raises the risks of the secure and economical operation of distribution networks (DNs) due to the intermittent wind speed and unexpected turbulence. To solve this problem, energy storage systems (ESSs) have received increasing attention for their advantages in smoothing power fluctuations induced by the wind power while reducing the impact of uncertain load demands in DNs through proper demand response (DR) designs [1–5]. In this context, this study presents a new approach to the optimal capacity allocation of ESSs in DN, which introduces a comprehensive DR to reduce the uncertainty of high-penetration WG and load demand using computational swarm intelligence.

Currently, several studies have explored solutions to accommodate the uncertainties from WGs and load demands. The uncertainty of wind power output has also been studied in the DN [6, 7]. In [8], WGs are precisely modeled in terms of time-scale and uncertainty to research the correlation of multiple time-scale, uncertainty, and simulation time. Simulation in a typical test system not only verifies the accuracy of the model proposed in this paper but also obtains the best prediction time-scale considering the simulation time and cost. In [9], a stochastic programming was used to model WGs to reduce the uncertainty in a home energy management. The simulation results demonstrate the home energy management with the WGs model can greatly reduce costs. Zhang et al. [10] proposed a novel wind prediction model based on particle swarm optimization and support vector machine (PSO-SVR) and grey combination model to reduce the disadvantage of low prediction accuracy of the traditional grey system. Compared with the single grey system, the mean absolute error (MAE), mean absolute

percentage error (MAPE), and root-mean-square error (RMSE) of the proposed model for WG prediction are improved by 37.7%, 34.9%, and 34.4%, respectively.

With the participation in DR programs, the roles of the consumers change from a passive entity to an active one that manages both local consumption and generation resources [11]. The authors in [12–14] studied the role of DR in load adjustment. In [12], a method is proposed to adjust the load curve considering the uncertainty of DR. Using the different acting speeds of the two types of DR, a two-stage scheduling model is established to reduce the uncertainty of load. The authors in [13, 14] proposed a new strategy using an optimal model of peak shaving and valley filling with electric vehicles for economic dispatching; the simulation results have demonstrated that the strategy is improving load management under large integration of electric vehicles (EVs). In [15], a DR optimization methodology for application in a generic residential house is proposed to find the optimal scheduling of minimal operating costs and reduce the uncertainty of load.

There are also many studies on stochastic optimization of wind power in DR. A stochastic programming investment model combining continuous operational constraints and wind scenarios was proposed in [16] to research the impact of DR in WGs. The numerical results show that, with the increase in DR capacity, wind power decreases and social surplus increases. In [17], a method was proposed to study the impact of WGs and DR on locational marginal prices. By shifting the proper amount of DR load from peak hours to off peaks, the utilization of WGs was enhanced and the investment cost was reduced. Ahmed et al. [18] analysed the impact of WGs on electricity price. The scenario simulation was conducted in Monte Carlo and then through the reduction and incorporation of scenarios to formulate stochastic uniform market price.

There have been some research efforts on the optimal configuration of ESSs to maintain the stability of the DN and reduce the uncertainty of WG and load demands furthermore in [19–23]. In [20], a novel planning model for the ESSs in distribution network wherein both load leveling and voltage profile improvement applications are extracted. Simulation results demonstrate that not only the load profile tends to be flat and resulting in lower energy cost but also the voltage profile can improve in some degrees without increasing planning and operation costs. ESSs can reduce power losses and improve the stability of a DN when ESSs were allocated at optimized locations in the network [21]. To ensure the minimum cost of substation expansion deferral, a novel multiobjective mixed integer linear programming model for ESSs operation was proposed in [22], and the proposed model is highly flexible with respect to the planner preferences, without increasing operation costs. Also, to accommodate the large penetration of wind energy, a multistep method based on the optimal power flow is presented in [23] for the configuration of ESSs to minimize the annual electricity cost in DNs.

Despite the extensive efforts, however, most of the works above relied on deterministic models to optimize ESS configuration in the DN. The deterministic models have not been able to consider the impact of load variations and adjustments under a comprehensive DR system nor the impact of the uncertainty of high WG penetration on the optimal capacity allocation of ESSs. To fill this gap, an optimal capacity allocation model of ESSs is proposed in this paper to minimize the cost and loss of ESSs under the conditions of secure and stable operation of DN and ESSs. In this new model, all objectives are incorporated in a single cost function to select the global optimal solution. The uncertainty of WG and load demands is modeled using particle swarm optimization and back-propagation (PSO-BP) neural network in a comprehensive DR, respectively, and an improved simulated annealing PSO (ISAPSO) algorithm is employed to optimize the ESS capacity allocation with minimized investment costs and energy losses. The main contributions of this paper are as follows:

(1) Proposing a new ESS optimal capacity allocation model to minimize the investment cost and power losses.

(2) ISAPSO is used to optimize the capacity allocation. Compared with another two algorithms proposed in this paper, the investment costs have been reduced by 12.5% and 7.1%, respectively, and the power losses have been reduced by 18.6% and 4.5%, respectively.

(3) A comprehensive DR system based on the time-of-use (TOU) and incentives are proposed to reduce the uncertainty of load.

(4) To predict the WGs more accurately, a PSO-BP neural network is proposed. Compared with the BP method, the MAE and RMSE of the proposed model for WG prediction is improved by 11.7% and 5.3%, respectively.

The rest of this paper is organized as follows. In Section 2, the ESS optimal capacity allocation model is first formulated, and the methodology to reduce the uncertainty of load demands and WG is introduced, respectively. In Section 3, the algorithms to solve the optimization model will be elaborated. The proposed model is evaluated on a modified 33-node test system under different conditions in Section 4. Finally, conclusions are drawn in Section 5.

2. Problem Formulation

The problem formulation is presented throughout this section to derive the model for optimal capacity allocation of ESSs. The problem formulation ideas for the entire paper is shown in Figure 1. The goal is to minimize the costs of investment and power losses, considering the uncertainty of load and wind generation, which is solved by the presented optimization model as a mixed-integer linear problem.

2.1. Objective Function. For ESSs, the objective function of the proposed optimization model can be given as

$$\min F = C_{\mathrm{INV}} + C_{\mathrm{LOSS}} + C_{\mathrm{DR}} - B_{\mathrm{shift}}, \tag{1}$$

where F is the total investment cost, C_{INV} is the life-time cost of ESS, C_{LOSS} is the cost of network loss, C_{DR} is the cost of implementing DR, and B_{shift} is the load adjustment profit.

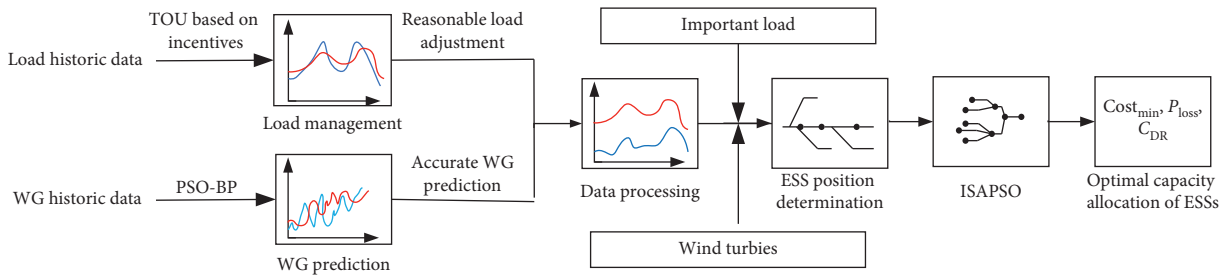

Figure 1: The overall idea of the method in this paper.

2.1.1. ESS Investment Cost. C_{INV}, the first term in equation (1), represents the life-time investment cost. It is defined as

$$C_{\mathrm{INV}} = \sum_{i=1}^{N}\left(c_E E_{\mathrm{ess},i} + c_P P_{\mathrm{ess},i}\right)\alpha + c_{\mathrm{om}} E_{\mathrm{ess},i}, \tag{2}$$

where N is the number of ESS installed, c_E is the unit capacity cost of ESS, c_P is the unit power cost of ESS, c_{om} is the unit O&M cost of ESS, and $E_{\mathrm{ess},i}$ and $P_{\mathrm{ess},i}$ are the capacity and power of the $i-$th ESS, respectively. Meanwhile, α is the transformation coefficient from the present value to a uniform annual value:

$$\alpha = \frac{\gamma_{\mathrm{ess}}\left(1+\gamma_{\mathrm{ess}}\right)^{l_{\mathrm{ess}}}}{\left(1+\gamma_{\mathrm{ess}}\right)^{l_{\mathrm{ess}}} - 1}, \tag{3}$$

where γ_{ess} is the interest rate and l_{ess} is the service life cycle of ESS.

2.1.2. Network Losses Cost. C_{LOSS}, the second term in equation (1), represents the costs of network power losses. It is defined as

$$C_{\mathrm{LOSS}} = \Delta t \sum_{i=1}^{N_L} c_{\mathrm{loss}} P_i, \tag{4}$$

where N_L is the total number of branches, c_{loss} is the unit power loss cost of the network, P_i is the power loss on the ith line, and Δt is the duration.

2.1.3. Cost of Implementing DR. C_{LOSS}, the third term in equation (1), represents the costs of the DR system. It is defined as

$$C_{\mathrm{DR}} = \sum_{i=1}^{N_L}\left(c_{\mathrm{DR}} P_{\mathrm{DR}} - c_0 P_0\right)\Delta t, \tag{5}$$

where c_{DR} and c_0 are the incentive and initial costs of unit power, respectively; P_0 and P_{DR} are the total power before and after implementing DR, respectively.

2.1.4. Load Adjustment Profit. B_{shift}, the benefits of load adjustments, can be calculated by the difference between the income from discharging the ESSs at peak hours and the cost of charging the ESSs at valley hours:

$$B_{\mathrm{shift}} = \sum_{i=1}^{N}\left(\lambda_{\mathrm{peak}} P_{\mathrm{dis},i} - \lambda_{\mathrm{offpeak}} P_{ch,i}\right)\Delta t, \tag{6}$$

where λ_{peak} and $\lambda_{\mathrm{offpeak}}$ are the peak and valley electricity prices, respectively; $P_{ch,i}$ and $P_{\mathrm{dis},i}$ are the charging and discharging power of the ith ESS, respectively.

2.2. Constraints

2.2.1. Power Balance Constraint

$$P_{\mathrm{WG},t} + P_{\mathrm{grid},t} + P^{d}_{\mathrm{bess},t} - P^{c}_{\mathrm{bess},t} = P_{\mathrm{load},t} + P_{\mathrm{loss},t}, \tag{7}$$

where $P_{\mathrm{WG},t}$ is the power of WGs at time t; $P_{\mathrm{grid},t}$ is the power purchased from the upper system at time t; $P^{c}_{\mathrm{bess},t}$ and $P^{d}_{\mathrm{bess},t}$ represent the charging and discharging power at time t, respectively; and $P_{\mathrm{load},t}$ and $P_{\mathrm{loss},t}$ represent the load power demand and network power loss at time t, respectively.

2.2.2. ESS Operational Constraint

$$\begin{cases} P^{c,t}_{\mathrm{bess},i} \le P^{c,\max}_{\mathrm{bess},i}, \\ P^{d,t}_{\mathrm{bess},i} \le P^{d,\max}_{\mathrm{bess},i}, \\ y^{c}_{\mathrm{bess},i} + y^{d}_{\mathrm{bess},i} \le 1, \\ \mathrm{SOC}^{t}_{\mathrm{bess},i} = \mathrm{SOC}^{t-1}_{\mathrm{bess},i} + \left(\dfrac{\eta_c P^{c}_{\mathrm{bess},i} - \left(1/\eta_d\right) P^{d}_{\mathrm{bess},i}}{P_{\mathrm{bess},i}}\right)\Delta t, \end{cases} \tag{8}$$

where $P^{c,t}_{\mathrm{bess},i}$ and $P^{d,t}_{\mathrm{bess},i}$ are the charging and discharging power of ESS at time t, respectively. $P^{c,\max}_{\mathrm{bess},i}$ and $P^{d,\max}_{\mathrm{bess},i}$ are the maximum charging and discharging power of ESS, respectively. $y^{c}_{\mathrm{bess},i}$ and $y^{d}_{\mathrm{bess},i}$ are the binary charging and discharging state of the ith ESS, respectively; η_c and η_d are the charging and discharging efficiency of the ESS, respectively.

2.2.3. Energy Balance Constraint of ESSs

$$\sum_{t=1}^{T} P^{c,t}_{\mathrm{bess},i}\eta_c \Delta t + \left(\frac{P^{d,t}_{\mathrm{bess},i}\Delta t}{\eta_d}\right) = 0. \tag{9}$$

2.3. Uncertainty Reduction. Due to the uncertainty of WG and load demand, it is difficult to obtain the optimal capacity allocation of ESSs at a high degree of accuracy. To reduce the impact of uncertainty on the proposed model, this study uses PSO-BP to improve the accuracy of WG prediction and use comprehensive DR to reduce the uncertainty of load demands based on load management.

2.3.1. WG Prediction Based on PSO-BP. Accurate WG prediction can improve the security and reliability of DN [24]. Current WG prediction methods include physical methods, statistical methods, and artificial intelligence methods. It is found that, among many WGs prediction methods, the PSO-BP neural network algorithm not only has a higher prediction accuracy but also reduce calculation time. So, the PSO-BP neural network algorithm is selected in this paper.

In the neural network, the data are first linearly normalized to the valid input range of the network. Then, we use the PSO algorithm to optimize the weights and bias of the BP neural network and improve the prediction accuracy. Given a BP neural network, the velocity and position s of each particle in the PSO are updated as follows:

$$\begin{cases} v_i^{l+1} = wv_i^l + c_1 r_1 \left(p_{\text{best}} - s_i^l\right) + c_2 r_2 \left(g_{\text{best}} - s_i^l\right), \\ s_i^{l+1} = s_i^l + v_i^{l+1}, \end{cases} \tag{10}$$

where l is the number of the current iteration; c_1 and c_2 are the cognitive factors and social factors, respectively; r_1 and r_2 are the random number distributed between [0, 1]; p_{best} is the individual optimal extremum; and g_{best} is the global optimal.

The total error of the samples is taken as the objective function as follows:

$$\begin{aligned} e_k &= \frac{1}{f} \sum_{i=1}^{f} \left(y_{k,i} - C_k\right)^2, \\ \text{fitness} &= \frac{1}{S} \sum_{k=1}^{S} e_k, \end{aligned} \tag{11}$$

where f is the total number of the actual values in sample k and S is the total number of the mean square errors in all samples. e_k, $y_{k,i}$, and C_k are the mean square error, the ith actual value, and the predicted value of sample k, respectively. The position of the optimal particle is used to assign the weight and bias of the corresponding neuron.

The normalized data are used as the input to the neural network, and the relationship between the input layer and the hidden layer is

$$z_j = \sum_{i=1}^{M} \omega_{ij} x_i' + b_j, \tag{12}$$

where x_i' is the input of the neuron i, z_j is the output of the neuron j, ω_{ij} is the weight of the link between neuron i and neuron j, b_j is the bias of neuron j, and M is the total number of neurons in the previous layer.

With the activation function, the relationship between the hidden layer and the output layer can be obtained as

$$y_j = \varphi\left(z_j\right), \tag{13}$$

where y_j is the output of the neuron j and $\varphi(x)$ is the activation function. In this paper, the Sigmoid function [25] is adopted, where $\varphi(x) = (1/1 + e^{-x})$.

Finally, the output power of the WGs is

$$P_{\text{WT}} = \frac{1}{2} c_p \rho A v^3, \tag{14}$$

where P_{WT} is the output power of WGs, c_p is the influencing factor of wind energy utilization coefficient of WGs, ρ is the air density, A is the swept air area, and v is the wind speed.

The root mean square error (RMSE) and mean absolute error (MAE) are used in the objective functions to evaluate the prediction performance of PSO-BP. Backpropagation and gradient descent algorithms are used to update the weights and bias to minimize the objective function [26].

2.3.2. TOU Model Based on Incentives. The uncertainty of load will affect the stability of DN dispatch due to the randomness of participating users' intentions. It is important for operators of DN to reduce the uncertainty of load [27]. Comprehensive DR generally refers to the use of both TOU and incentive measures for load management. According to the research, comprehensive DR has better performance than using TOU or incentive measures alone [28, 29]. So, we choose comprehensive DR as the approach to reduce the load uncertainty.

In DR, the relationship between users' load and electricity price is usually described using the demand elasticity coefficient (DEC) as follows:

$$\begin{aligned} \lambda_{ij} &= \frac{\Delta l_{ij}/l_{i0}}{\Delta l_{ij}/l_{i0}}, \\ \Delta l_{ij} &= l_j - l_{i0}, \\ \Delta p_{ij} &= p_j - p_{i0}, \end{aligned} \tag{15}$$

where Δl_{ij} is the load difference between time j and time i; Δp_{ij} is the electricity price difference between time j and time i; l_{i0} and p_{i0} represent the load and electricity price before DR, respectively; and l_j and p_j represent the load and electricity price of the period j after the DR, respectively.

When i and j are not equal, λ_{ij} represents the cross DEC in different periods: when the electricity price at time j is low and the load at time i is shifted to time j, the DEC is positive. When i and j are the same, λ_{ij} represents time i own self-elastic coefficient: when the price of electricity rises, the load of time i will be shifted to other periods and thus the DEC is negative. A DEC matrix E can be then composed of the self-elastic and mutual elastic coefficients:

$$E = \begin{bmatrix} \lambda_{11} & \lambda_{12} & \cdots & \lambda_{1M} \\ \lambda_{21} & \lambda_{22} & \cdots & \lambda_{2M} \\ \vdots & \vdots & \vdots & \vdots \\ \lambda_{M1} & \lambda_{M2} & \cdots & \lambda_{MM} \end{bmatrix}, \tag{16}$$

where M represents the periods divided in one day. The main diagonal elements are self-elastic coefficients, while the others are mutual elastic coefficients. This DEC matrix can be obtained from the historical TOU data.

Once E is obtained, the load matrix L in each period can be calculated from the historical TOU data:

$$L = \begin{bmatrix} l_1 \\ l_2 \\ \vdots \\ l_T \end{bmatrix} = \begin{bmatrix} l_{10} & 0 & \cdots & 0 \\ 0 & l_{20} & 0 & 0 \\ \vdots & \vdots & \vdots & \vdots \\ 0 & 0 & \cdots & l_{T0} \end{bmatrix} E \begin{bmatrix} \dfrac{\Delta p_1}{p_{10}} \\ \dfrac{\Delta p_2}{p_{20}} \\ \vdots \\ \dfrac{\Delta p_T}{p_{T0}} \end{bmatrix} + \begin{bmatrix} l_{10} \\ l_{20} \\ \vdots \\ l_{T0} \end{bmatrix}. \tag{17}$$

The optimized load model can be obtained by adding the following incentive mechanism based on the load matrix defined above:

$$L = \begin{bmatrix} l_{10} & 0 & \cdots & 0 \\ 0 & l_{20} & 0 & 0 \\ \vdots & \vdots & \vdots & \vdots \\ 0 & 0 & \cdots & l_{T0} \end{bmatrix} \left(D_1 \begin{bmatrix} \dfrac{\Delta p_1 + a_1}{p_{10}} \\ \dfrac{\Delta p_2 + a_2}{p_{20}} \\ \vdots \\ \dfrac{\Delta p_T + a_T}{p_{T0}} \end{bmatrix} + D_2 \begin{bmatrix} \dfrac{\Delta p_1 + a_{j1}}{p_{10}} \\ \dfrac{\Delta p_2 + a_{j2}}{p_{20}} \\ \vdots \\ \dfrac{\Delta p_T + a_T}{p_{T0}} \end{bmatrix} \right) + \begin{bmatrix} l_{10} \\ l_{20} \\ \vdots \\ l_{T0} \end{bmatrix}, \tag{18}$$

where $D_1 = \mathrm{diag}[\lambda_{11}, \lambda_{22}, \ldots, \lambda_{TT}]$ is the main diagonal of the DEC matrix, that is, the matrix of self-elastic coefficients; $D_2 = E - D_1$ is the matrix of mutual elasticity coefficients, a_T is the incentive value at time period T, and a_{jT} is the incentive value to which the load is shifted.

3. Solving the Optimization Model

From a mathematical perspective, the proposed model is a nonlinear commitment optimization problem with mixed integers. To tackle the challenge, PSO-BP is used for WG prediction, and adjustable activation function and embedding chaos algorithm (BP-AAEC) is used for reducing the uncertainty of load demands based on reasonable load management. Then, ISAPSO is adopted to satisfy the demands of efficiency and convergence. The optimization solution mainly includes the following steps:

(1) WGs prediction

Step 1.1: generate an initial population of PSO-BP. The number of hidden nodes and the initial connection density for each network are generated. And normalize the original WGs data.

Step 1.2: according to the input vector, the weight between an input-layer neuron and hidden-layer neuron ω_{ij} evaluates the output values of hidden layer by equation (12). Calculate the output values of output layer based on the weight between output-layer neuron and hidden-layer neuron bias b_j by equation (13).

Step 1.3: initialize the position of each particle of PSO by means of weight ω_{ij} and bias b_j by equation (10). Evaluate the new fitness and update the global optimum.

Step 1.4: update the weight and bias according to an iterative number of PSO algorithm. The optimal parameters obtained by PSO are given to the BP neural network model.

Step 1.5: if $t < t_{\max}$, then $t = t + 1$, and go back to Step 1.4; otherwise, output the predictive result.

(2) Load scheduling

Step 2.1: initialize BP-AAEC and set the initial value of each parameter. Normalize the historical load data. Suppose the weight value is ω and bias is b. Let e be the error function threshold; set the initial value of the parameter as X_0. Let X^* be the most optimum network parameter at present $X^* = X_0$.

Step 2.2: run BP-AAEC and get the parameter X_k^*; let $k = k + 1$.

Step 2.3: evaluate the fitness in equation (17) and compare $f(X_k^*)$ with $f(X^*)$.

Step 2.4: calculate $\Delta f = f(X_k^*) - f(X^*)$: if $\Delta f < e$, the prediction is convergent. If $\Delta f > e$, return to Step 2.2.

(3) Optimal capacity allocation of ESSs

Step 3.1: initialize the population of ISAPSO, including the position, velocity, and initial temperature.

Step 3.2: calculate the fitness by equation (1), with the constraint equations (7)–(9).

Step 3.3: update the velocity and position by equation (10).

Step 3.4: calculate the new fitness in equation (1) for each particle.

Step 3.5: apply the annealing $T_{k+1} = \lambda T_k$.

Step 3.6: if the iteration conditions are met, stop the search; otherwise, return to Step 3.3.

The flowchart of the entire algorithm is shown in Figure 2.

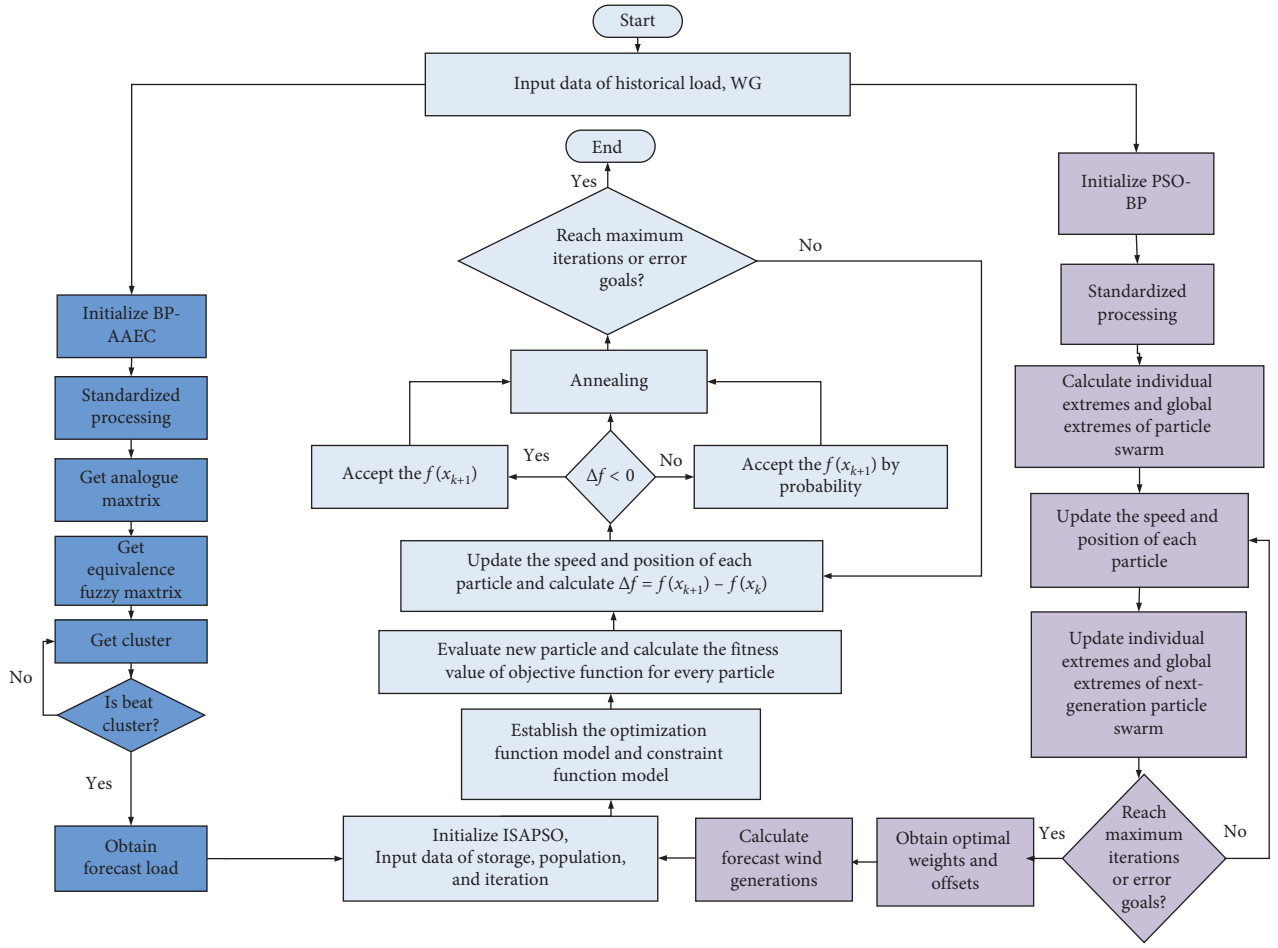

Figure 2: The optimization procedure for finding optimal planning schemes.

4. Case Study

4.1. Benchmark System. The proposed method is evaluated on a modified IEEE 33-node test distribution system, as illustrated in Figure 3 [30]. The rated voltage of the system is 12.6 kV with a peak load of 3.775 + j2.300 MVA. The important loads are set on Nodes 3, 10, and 26. In order to serve the important loads continuously when the DN fails and to ensure the stability of the system, the WGs are allocated in Node 4 (800 kW) and Node 14 (1000 kW), where the power factor is 0.8. The rated cut-in and cut-out wind speeds are 12 m/s, 4 m/s, and 20 m/s, respectively.

The heuristic algorithm selected in this paper can be applied for different types of ESSs, such as the lead-acid battery (LAB), the sodium-sulfur battery (NaS), or the Li-ion battery (LIB), among others [31]. The parameters of the three types of batteries are provided in Table 1 [32]. Considering the service life and costs of investment, the sodium-sulfur battery is used. Also, considering the important loads and the stable operation of the DN, we assumed ESSs are allocated in Nodes 2, 6, and 12. The rest parameters refer to Table 2, and the other parameters of ESSs are the same as in Table 1. The price of electricity in different time periods and the incentive value are shown in Figure 4.

4.2. Comparison of Simulation Results. In the ISAPSO, the number of population particles and iterations are set as 30 and 100, respectively. To evaluate the performance, the following cases are considered:

Case A: simulation of the IEEE-33 system of considering reducing the uncertainty of WGs and load, without ESSs

Case B: optimize the capacity allocation of ESSs by only reducing the uncertainty of load, and the output of WGs is simply the rated power

Case C: optimize the capacity allocation of ESSs by only reducing the uncertainty of WGs and DR is not adopted to reduce the uncertainty of load

Case D: optimize the capacity allocation of ESSs by reducing the uncertainties of WGs and load by the means of this paper proposed

The simulation results are shown in Figure 5. In the absence of ESSs, even if the method of reducing the uncertainty of WGs and load mentioned in this paper is used in the simulation, there will be greater power loss and voltage deviation. Compared with Case A and Case B, although the comprehensive DR can introduce some costs in Case C, it improves the effect of load shifting and reduces the power

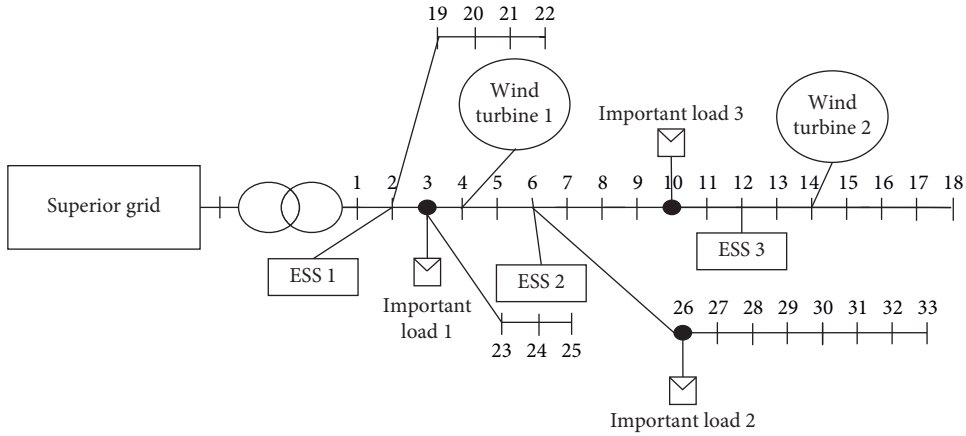

Figure 3: The modified IEEE 33-bus distribution test system.

Table 1: Comparison of three different batteries.

Parameter	LAB	NaS	LIB
Fixed O&M (¥/kW)	25.5	27	51.75
Efficient (%)	80	85	90
Range of SOC (%)	30–70	10–90	20–80
Service life (years)	10	15	12.5

Table 2: Parameters of the simulation.

Parameter	Value
Number of charge/discharge cycles in storage life	10000
ESSs investment cost (¥/kWh)	1000
Interest rate	3%
Annual increment load rate	10%
Power loss cost (¥/kWh)	0.4

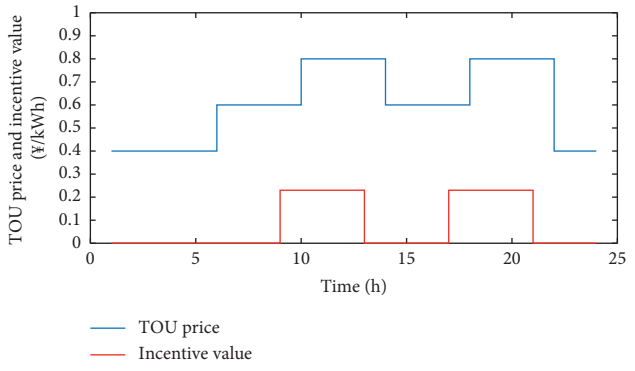

Figure 4: Elasticity coefficient of TOU electricity price and incentive value.

losses (18.4% and 4.5%, respectively). Overall, Case C can reduce the uncertainty of load and WGs at the same time, making the DN more stable at a lower total cost of investment (12.5% and 7.1%, respectively) than Case A and Case B.

Simultaneously, in order to prove that the position of ESSs and WGs selected in this paper is optimal, the following cases are performed:

Case A: optimize the capacity allocation of ESSs considering only changing the location of ESSs (they are set on Nodes 11, 19, and 27, respectively), and the positon of WGs does not change.

Case B: optimize the capacity allocation of ESSs considering only changing the location of WGs (they are set on Nodes 7 and 16, respectively), and the positon of ESSs does not change.

Case C: optimize the capacity allocation of ESSs considering changing the location of ESSs (they are set on Nodes 11, 19, and 27, respectively) and WGs (they are set on Nodes 7 and 16, respectively), simultaneously.

Case D: optimize the capacity allocation of ESSs according to the location of ESSs and WGs provided in this paper.

The above simulation cases are all based on the methods proposed in this paper, and the selection of nodes is random. Table 3 presents comparison of the above four cases. As we can observed from Table 3, both the power losses and the voltage deviation of the DN will be increased when the location of the ESSs or the WGs changes. This is because the change in position makes the role of ESSs or WGs unable to radiate the entire DN, which increases the cost of ESSs and reduces the stability of the distribution network. Therefore, only when the optimal location is selected for ESSs and WGs in the DN can the cost and stability be minimized.

4.3. Comparison of Different Algorithms. To evaluate the performance of the proposed algorithm, the section will first verify the feasibility of the proposed method to reduce the uncertainty of load demands and WGs prediction, respectively. After that, the validity of the optimal capacity allocation model is validated by comparing it with other methods. Finally, in order to prove the superiority of IASPSO, this paper selected PSO and NSGA-II to compare with ISAPSO.

4.3.1. Comparison of Uncertainty Reduction. To illustrate the effectiveness of the proposed method, the uncertainty of load

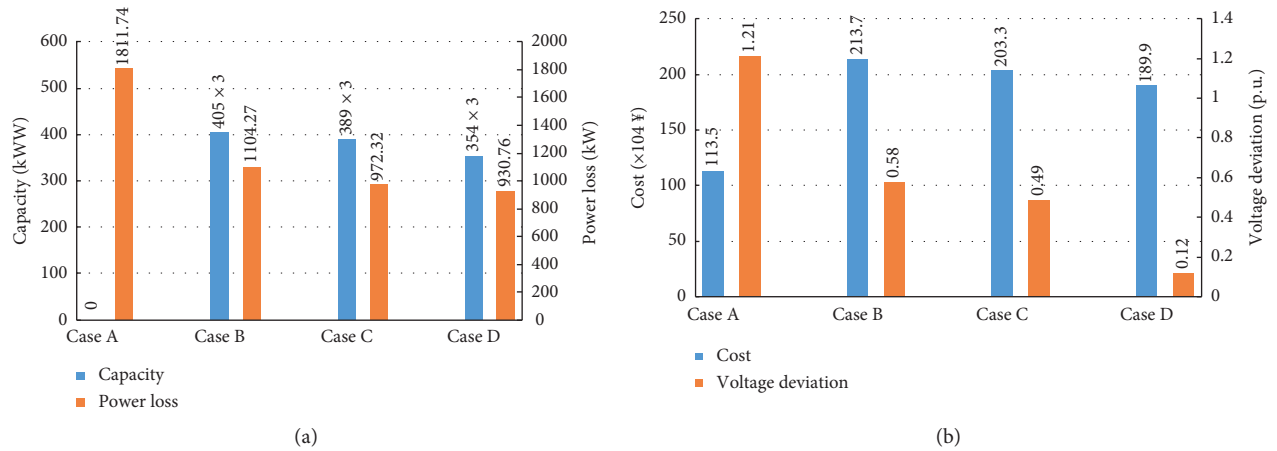

(a) (b)

Figure 5: Comparison of optimization results of different schemes.

Table 3: Simulation results of the above four cases.

Parameter	Case A	Case B	Case C	Case D
Capacity of ESSs (kW)	372×3	369×3	398×3	354×3
Power losses (kW)	987.17	970.33	1011.25	930.76
Cost ($\times 10^4$ yuan)	202.7	193.8	209.1	189.9
Voltage deviation (rad p.u.)	0.44	0.48	0.63	0.12

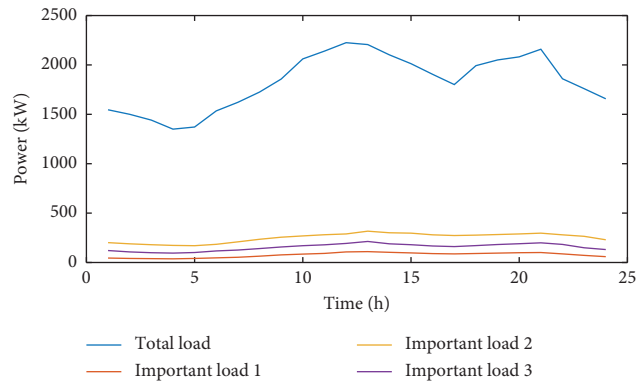

Figure 6: Daily load curves of total load and important load.

and WGs proposed in this paper is firstly evaluated. Two typical cases will be considered: Case 1 only considers load scheduling under TOU tariff, while Case 2 considers TOU based on incentives. The historical data of the total load and each important load are shown in Figure 6. And the load adjustment under the two different DRs is shown in Figure 7. It can be seen from the figure that the shifting load in the second case is better.

As shown in Figure 7, we can see that the peak load decreases, valley load rises, and the difference between peak and valley decreases when we adopt the strategy of case 1. For a part of the load that cannot be transferred during the period, the peak-to-valley difference can decrease further by the strategy of case 2 while giving some compensation and the load curve is more smooth. This is because case 2 adopts an TOU based on incentives strategy to enable load adjustment with the participation of the distribution network operator, which allows the load to be further adjusted compared to case 1. The detailed peak-to-valley difference is shown in Table 4.

DGs have a great impact on the stability of the DN. In order to ensure the stable operation of the system, it is necessary to reduce the uncertainty of DGs. In this part, we will prove the effectiveness of the proposed method to reduce the uncertainty of DGs by comparing BP with the PSO-BP. The historical data of the total DGs and each DG are shown in Figure 8.

The comparison of PSO-BP and BP WGs prediction is shown in Figure 9. We can see from Figure 9 that both of the two prediction methods have high precision but PSO-BP has better prediction accuracy than BP. This is because BP adopts error backpropagation to adjust the weight of network connection, and it is easy to fall into the local optimal solution, while PSO-BP can search in a larger space, which avoids the above problem to a certain extent, so that the prediction accuracy has been further improved.

The MAE and RMSE of total DGs are applied to evaluate the predicted results. As can be seen in Table 5, compared with the BP method, the MAE and RMSE of the proposed model for WG prediction is improved by 11.7% and 5.3%, respectively. Therefore, the method proposed in this paper can greatly reduce the uncertainty of WG prediction.

Table 6 shows the comparison of ISAPSO and PSO and NSGA-II. Among these three algorithms, the calculation time of ISAPSO is longer than PSO because ISAPSO requires a simulated annealing process. Since the calculation process of NSGA-II is different, no comparison of calculation time is performed. ISAPSO has a better performance in global search than PSO due to the addition of a simulated annealing process. The results have shown that ISAPSO reduces the costs of both the investment (6.7%, 1.3%) and power loss (41.9%, 82.8%). In terms of voltage deviation, compared with PSO and NSGA-II, the voltage deviation calculated by ISAPSO was reduced by 0.20 and 0.06 p.u., respectively. Because ISAPSO has better global search capabilities than PSO, it has better simulation results. As for the comparison with NSGA-II, because ISAPSO has the "memory function" that NSGA-II does not have, the search results are relatively

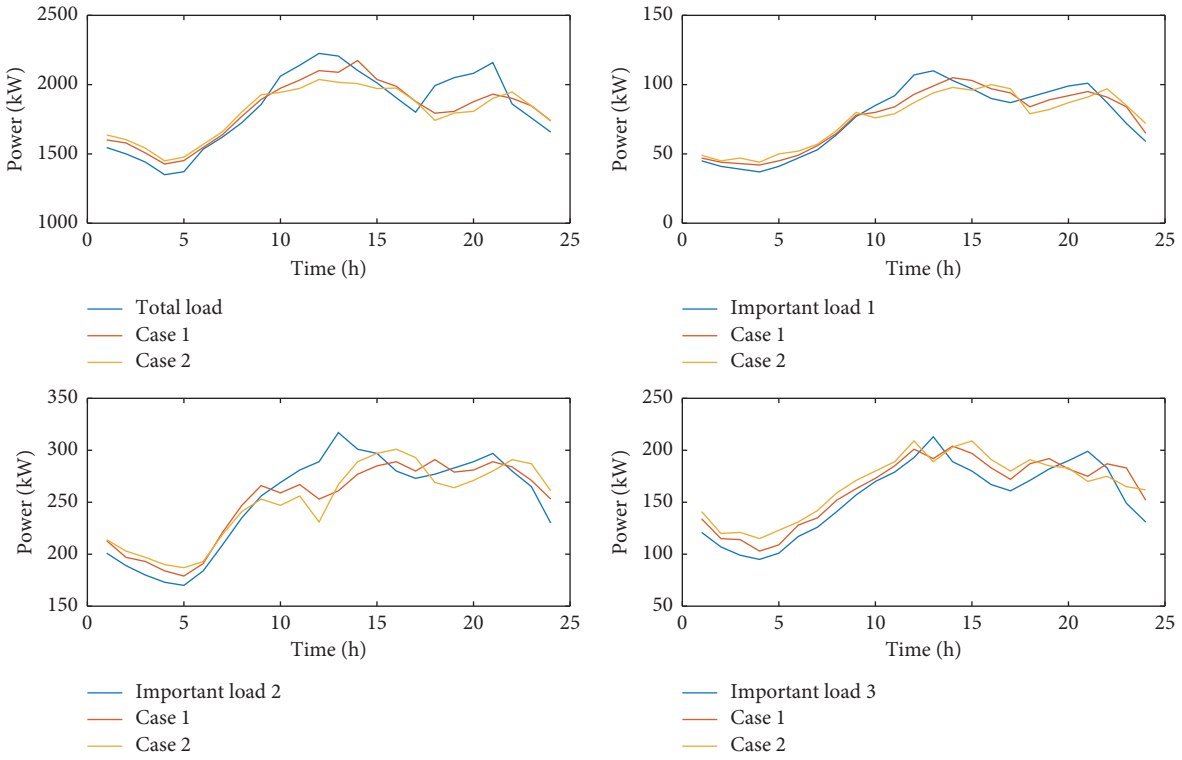

Figure 7: Comparison of different load adjustment strategies.

Table 4: Comparison of peak-to-valley difference under different strategies.

Parameter	The original data	Case 1	Case 2
Total load	875	747	587
Important load 1	73	63	56
Important load 2	147	114	110
Important load 3	118	100	94

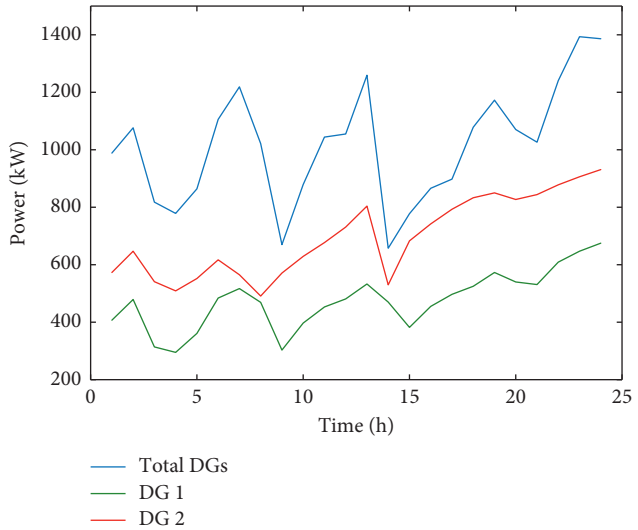

Figure 8: Daily DGs curves of total DG and points load.

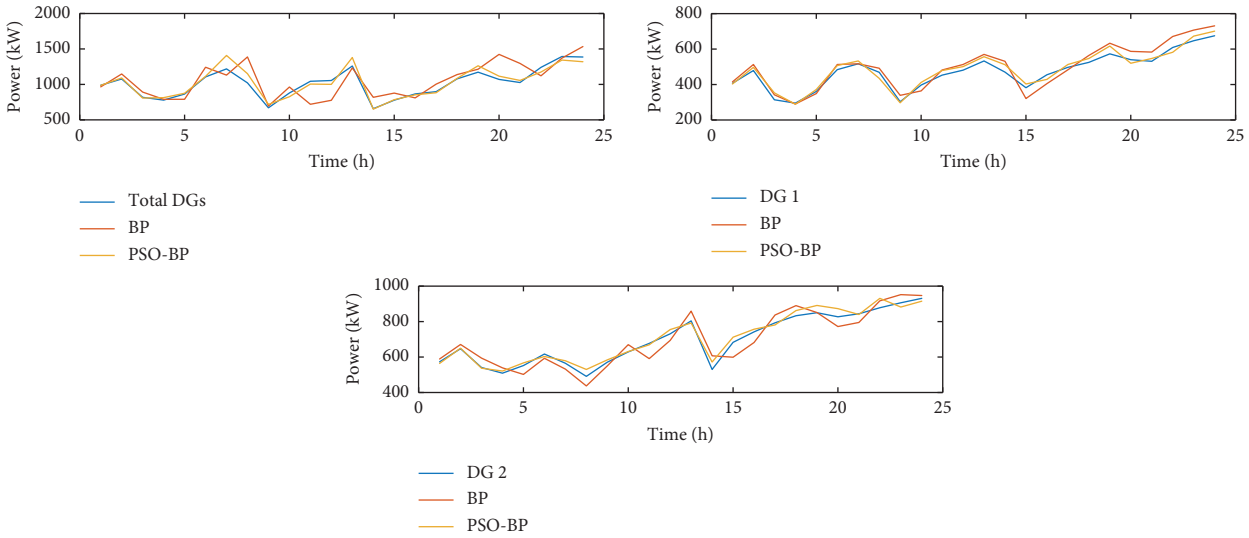

Figure 9: Comparison of different DGs prediction strategies.

Table 5: Comparison of error indicator.

Parameter	BP	PSO-BP
MAE	0.1494	0.1337
RMSE	0.1715	0.1628

Table 6: Comparison of different algorithm.

	PSO	NSGA-II	ISAPSO
Power losses (kW)	1321.01	1701.00	930.76
Cost ($\times 10^4$ yuan)	202.7	192.4	189.9
Voltage deviation (rad p.u.)	0.32	0.18	0.12
Time (S)	13.810	52.820	18.967

better. Therefore, ISAPSO offers a better solution to the optimal capacity allocation model in this paper.

4.4. Sensitive Analysis for Incentives. Table 4 gives the results of sensitive analysis conducted for the DN stability considering electricity price incentive factors. As it can be observed, by adjusting load management measures and wind power forecasting methods, the power loss of the distribution network and the capacity and cost of the ESS will change accordingly. As shown in Figure 7, when incentives are added to the TOU, the DNs total load peak-to-valley difference is reduced by 21.42% compared to when only the TOU is applied. Incentives are more like an administrative measure, which also shows that when administrative measures are added to the DN, it will be more helpful to the stability of the power grid.

5. Conclusions

This paper proposed an optimal capacity allocation scheme for ESSs by reducing the influence of uncertainty of WGs and load demands in DNs. Furthermore, the combination of comprehensive DR and PSO-BP reduced the uncertainty of load demands and WG, respectively. The optimal capacity allocation of ESSs is solved by a cost-benefit analysis considering the reduction of power losses and load shift.

In order to prove the generality of our model, we first compared the TOU with the comprehensive DR proposed in this paper for the load adjustment method. Based on the simulation results, the comprehensive DR has better performance in reducing the uncertainty of load than TOU with a slightly increased cost than the latter. Then, we compared BP with PSO-BP for more accurate DGs prediction. From the obtained results, we can see that the PSO-BP is more accurate than BP for WG prediction. The MAE and RMSE are 0.1337 and 0.1628 in PSO-BP and 0.1494 and 0.1715 in BP, respectively. Finally, we got the optimal capacity allocation of ESSs by the ISAPSO algorithm. The simulation results show that the optimal capacity allocation model of ESSs can better reduce the cost of investment and power losses and improve the stability of DNs when we combine the comprehensive DR and PSO-BP instead of using only one of them. Furthermore, the proposed algorithm can reduce the computation time and obtain better results than other heuristic algorithms.

For the future work, along with the expected continuing development in battery technology, we will choose batteries with better performance as the ESSs of the DN. In addition, the holidays and weather conditions will also be considered. And more efficient heuristic algorithms will also be used to solve the optimal allocation model of ESSs.

Data Availability

The data used to support the findings of this study are available from the corresponding author upon request.

Conflicts of Interest

The authors declare that there are no conflicts of interest.

Acknowledgments

This research was supported by the National Key Research and Development Program of China (no. 2017YFB0903300), Research Program of State Grid Corporation of China (no. SGTYHT/16-JS-198), and National Natural Science Foundation of China (no. 51807134).

References

[1] X. Zhang, M. Shahidehpour, A. Alabdulwahab, and A. Abusorrah, "Optimal expansion planning of energy hub with multiple energy infrastructures," *IEEE Transactions on Smart Grid*, vol. 6, no. 5, pp. 2302–2311, 2015.

[2] Y. Zhang, K. Meng, F. Luo, Z. Y. Dong, K. P. Wong, and Y. Zheng, "Optimal allocation of battery energy storage systems in distribution networks with high wind power penetration," *IET Renewable Power Generation*, vol. 10, no. 8, pp. 1105–1113, 2016.

[3] C. Chen, B. Que, and L. Ge, "Cost-benefit analysis of distributed energy storage in distribution grids with renewables," in *Proceedings of the 2018 International Conference on Power System Technology*, Guangzhou, China, November 2018.

[4] P. Siano, "Demand response and smart grids-a survey," *Renewable and Sustainable Energy Reviews*, vol. 30, no. 2, pp. 461–478, 2014.

[5] Y. Dong, Z. Zhang, and W.-C. Hong, "A hybrid seasonal mechanism with a chaotic cuckoo search algorithm witha support vector regression model for electric load forecasting," *Energies*, vol. 11, no. 4, 2018.

[6] L. Xiao, F. Qian, and W. Shao, "Multi-step wind speed forecasting based on a hybrid forecasting architecture and an improved bat algorithm," *Energy Conversion and Management*, vol. 143, pp. 410–430, 2017.

[7] S. Fang and H.-D. Chiang, "A high-accuracy wind power forecasting model," *IEEE Transactions on Power Systems*, vol. 32, no. 2, pp. 1589-1590, 2017.

[8] H. Mehrjerdi and E. Rakhshani, "Correlation of multiple time-scale and uncertainty modelling for renewable energy-load profiles in wind powered system," *Journal of Cleaner Production*, vol. 236, pp. 1–8, 2019.

[9] H. Mehrjerdi and R. Hemmati, "Coordination of vehicle-to-home and renewable capacity resources for energy management in resilience and self-healing building," *Renewable Energy*, vol. 146, pp. 568–579, 2020.

[10] Y. Zhang, H. Sun, and Y. Guo, "Wind power prediction based on PSO-SVR and grey combination model," *IEEE Access*, vol. 7, pp. 136254–136267, 2019.

[11] C. Roldán-Blay, G. Escrivá-Escrivá, and C. Roldán-Porta, "Improving the benefits of demand response participation in facilities with distributed energy resources," *Energy*, vol. 169, pp. 710–718, 2019.

[12] S. Sheng and Q. Gu, "A day-ahead and day-in decision model considering the uncertainty of multiple kinds of demand response," *Energies*, vol. 12, no. 9, p. 1711, 2019.

[13] X. Sun, X. Bai, and L. Liu, "Multi-objective planning for electric vehicle charging stations considering TOU price," in *Proceedings of the 2017 3rd IEEE International Conference on Cybernetics*, pp. 21–23, Exeter, UK, June 2017.

[14] H. Liang, Y. Liu, F. Li, and Y. Shen, "Dynamic economic/emission dispatch including PEVs for peak shaving and valley filling," *IEEE Transactions on Industrial Electronics*, vol. 66, no. 4, pp. 2880–2890, 2019.

[15] R. Faia, P. Faria, Z. Vale, and J. Spinola, "Demand response optimization using ParticleSwarm algorithm considering optimum battery energy storage schedule in a residential house," *Energies*, vol. 12, no. 9, 2019.

[16] S. Jin, A. Botterud, and S. M. Ryan, "Impact of demand response on thermal generation investment with high wind penetration," *IEEE Transactions on Smart Grid*, vol. 4, no. 4, pp. 2374–2383, 2013.

[17] Z. Zhao and L. Wu, "Impacts of high penetration wind generation and demand response on LMPs in day-ahead market," *IEEE Transactions on Smart Grid*, vol. 5, no. 1, pp. 220–229, 2014.

[18] M. H. Ahmed, K. Bhattacharya, and M. M. A. Salama, "Stochastic analysis of wind penetration impact on electricity market prices," in *Proceedings of the 2011 IEEE Power and Energy Society General Meeting*, IEEE, pp. 1–8, Detroit, MI, USA, July 2011.

[19] H. Mehrjerdi, "Multilevel home energy management integrated with renewable energies and storage technologies considering contingency operation," *Journal of Renewable and Sustainable Energy*, vol. 11, no. 2, 2019.

[20] H. Mehrjerdi, "Simultaneous load leveling and voltage profile improvement in distribution networks by optimal battery storage planning," *Energy*, vol. 181, pp. 916–926, 2019.

[21] Y. Yao, D. Liu, and H. Liao, "Analysis on loss reductionof distribution network with energy storage battery," *East China Electric Power*, vol. 5, pp. 677–680, 2010.

[22] H. Mehrjerdi, E. Rakhshani, and A. Iqbal, "Resilience-uncertainty nexus in building energy management integrated with solar system and battery storage," *IEEE Access*, vol. 27, p. 1, 2020.

[23] S. Wen, H. Lan, Q. Fu, D. C. Yu, and L. Zhang, "Economic allocation for energy storage system considering wind power distribution," *IEEE Transactions on Power Systems*, vol. 30, no. 2, pp. 644–652, 2015.

[24] S. Wang, X. Zhang, L. Ge, and L. Wu, "2-D wind speed statistical model for reliability assessment of microgrid," *IEEE Transactions on Sustainable Energy*, vol. 7, no. 3, pp. 1159–1169, 2016.

[25] A. Yang, Y. Zhuansun, C. Liu, J. Li, and C. Zhang, "Design of intrusion detection system for internet of things based on improved BP neural network," *IEEE Access*, vol. 7, pp. 106043–106052, 2019.

[26] S. Wan and L. Banta, "Parameter Incremental learning algorithmfor neural networks," *IEEE Transactions on Neural Networks*, vol. 17, no. 6, pp. 1424–1438, 2006.

[27] M. Paulus and F. Borggrefe, "The potential of demand-side management in energy-intensive industries for electricity markets in Germany," *Applied Energy*, vol. 88, no. 2, pp. 432–441, 2011.

[28] W. Zhu, Z. Liao, and H. Liu, "Expansion programming method for active distribution networks consideringdemand response and high ratio of renewable energy access," in *Proceedings of the Chinese Society for Electrical Engineering*, Shenyang, China, September 2019.

[29] M. Lei, W. Wei, and J. Zeng, "Effect of load control on power supply reliability considering demand response," *Automation ofElectric Power Systems*, vol. 42, no. 10, pp. 53–59, 2018.

[30] R. Ranjan and D. Das, "Simple and efficient computer algorithm to solve radial distribution networks," *Electric Power Components and Systems*, vol. 31, no. 1, pp. 95–107, 2003.

[31] B. Zakeri and S. Syri, "Electrical energy storage systems: a comparative life cycle cost analysis," *Renewable and Sustainable Energy Reviews*, vol. 42, pp. 569–596, 2015.

[32] R. Li, W. Wang, Z. Chen, and X. Wu, "Optimal planning of energy storage system in active distribution system based on fuzzy multi-objective bi-level optimization," *Journal of Modern Power Systems and Clean Energy*, vol. 6, no. 2, pp. 342–355, 2018.